A&A 425, 553–567 (2004)
DOI: 10.1051/0004-6361:20034352


Astronomy & Astrophysics

# Sharpless 170 and the surrounding interstellar medium

R. S. Roger[1], W. H. McCutcheon[2], C. R. Purton[1], and P. E. Dewdney[1]

[1] National Research Council Canada, Herzberg Institute of Astrophysics, Dominion Radio Astrophysical Observatory, Penticton, BC V2A 6J9, Canada
e-mail: robert.roger@hia.nrc.ca
[2] Department of Physics and Astronomy, University of British Columbia, Vancouver, BC V6T 1Z1, Canada

Received 18 September 2003 / Accepted 17 June 2004

**Abstract.** Sharpless 170 is a diffuse HII region ionized by a single main sequence O-star located near the periphery of a small dense molecular cloud at a distance of ~2 kpc. We describe wide-field observations of the region in the radio continuum, in HI and CO-lines, and in the far-infrared which delineate the major ionized, atomic, molecular and dust components of the gas affected by the exciting star. From the thermal continuum emission we estimate the mass of ionized gas at ~350 $M_\odot$ within a radius of ~7 pc. The HI ($\lambda$21 cm) and far-infrared observations show an extended low-density atomic component, of ~1000 $M_\odot$, within an irregular boundary surrounding the ionized gas of mean radius ~10 pc. Mean densities in the HI and HII are similar, in the range 9–16 nucleons cm$^{-3}$. CO emission shows a molecular cloud of ~1150 $M_\odot$ within an area 6 pc × 4 pc with densities ~2000 nucleons cm$^{-3}$. A compact infrared component coincides with the cloud. The exciting star is located on the near side of the cloud, just inside the southern periphery.
Sh170 is an example of a young HII region with the ionized gas, seen in H$\alpha$ emission, streaming outward in the manner of a "champagne flow". Although the observed velocities of the HI are close to the mean velocity of the CO cloud, the morphology of the associated atomic hydrogen closely resembles that seen in the surrounds of other young HII regions which show clear evidence of expansion of their HI. We propose that much of the HI is a diffuse dissociation zone beyond the ionization front, in directions from the star within a wide annulus, approximately transverse to the line-of-sight, between the dense photon-bounded region on the far side of the star and the density-bounded ionized flow region on the near side. In this view, much of the associated atomic gas, like the ionized gas, has been eroded from the molecular cloud in a small fraction (≤10%) of the star's main sequence lifetime.

**Key words.** stars: individual: BD +63 2093p (AG+64 1262) – Galaxy: open clusters and associations: individual: Sh 2-170 – radio continuum: ISM – radio lines: ISM – infrared: ISM

## 1. Introduction

Ultraviolet emissions from O and early-B stars dissociate, ionize and heat the parent molecular clouds and nearby intercloud gas. Through these processes, newly-formed massive O stars can seriously disrupt surrounding cloud condensations and initiate a complete re-distribution of cloud and intercloud material. The large-scale evolution of such star-forming regions and their surroundings is dependent primarily upon the stellar luminosity and upon the density and distribution of the surrounding gas and dust. A comprehensive understanding of the evolution and of the detailed photo-dynamic and photo-chemical processes at work requires a testing of theory and models against multi-wavelength observations of star-forming regions displaying a wide variety of conditions.

Observations of isolated molecular clouds with a single source of excitation and HII-region are ideal for studies of the gross properties of the various components of gas and dust. Several such regions have been observed and their properties are summarized by Roger & Dewdney (1992) in a paper which describes models of the evolution of the dissociation and ionization of the molecular hydrogen surrounding newly formed O and early-B stars. More recent models of the development of similar photo-dissociation regions are those of Bertoldi & Draine (1996) and Diaz-Miller et al. (1998). The current knowledge of the processes in, and evolution of photo-dissociation regions in general has been reviewed by Hollenbach & Tielens (1999).

Sharpless 170 is a faint, almost circular HII region in Cassiopeia ($l$ = 117.62°, $b$ = +2.27°) with an angular diameter of approximately 18′. The nebula is excited by a single, centrally located main-sequence O star, BD +63 2093p (AG+64 1262, LS I +64 11), which is a member of a small open cluster, Stock 18. The cluster is at a photometric distance of 2.2 ± 0.4 kpc (D. Turner, personal communication; Mayer & Macák 1973). Figure 1 shows the faint emission from Sh170 as depicted on the E-plate of the Palomar Sky Survey. Over most of the periphery the outline of the emission is not well

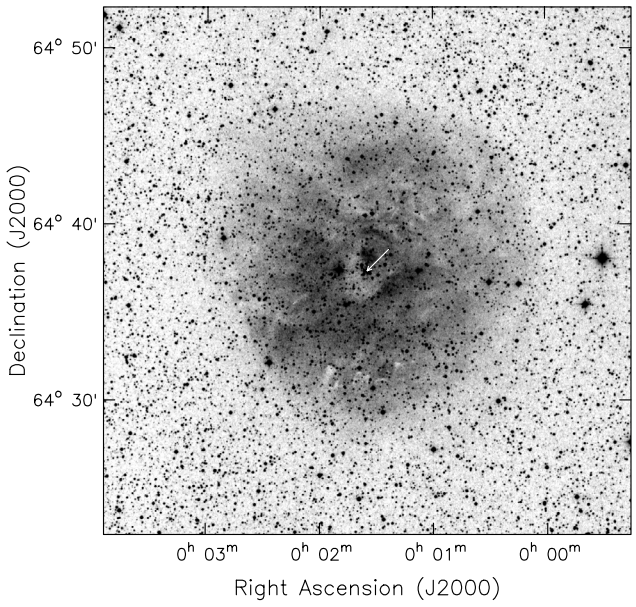


**Fig. 1.** A 0.5° field from the digitized images of the POSS E-plate, centred on Sh170. An arrow points to the position of the exciting star.

defined, implying that the nebula is density limited in these directions. An exception to this occurs on the south-east side. A few patches or knots of obscuration are also visible, particularly in the south and south-east. There is also a central depression in emission centred slightly to the southeast of the exciting star. Miville-Duchênes et al. (1995) have shown that this feature is probably a stellar wind cavity.

The single exciting star has been variously classified, spectroscopically, as O8V (Hunter & Massey 1990) and O9V (Mayer & Macák 1973; Crampton & Fisher 1974) and, photometrically, as O9V (Felli & Harten 1981) and O9.5V (Georgelin et al. 1973; Lahulla 1985). We will assume a classification of O9V. The four next most luminous stars in Stock 18 are classified in the range B8V–B9V.

We have mapped a region centred on Sh170 in HI-line and continuum emission at $\lambda$21 cm using the Synthesis Telescope at the Dominion Radio Astrophysical Observatory[1]. Also, we have mapped the emission of two isomers of CO from the molecular cloud associated with Sh170, using the 4.9-m telescope at the Millimeter Wave Observatory (MWO) of the University of Texas.

The HI/HII complex is readily apparent in the far-infrared emission detected by the IRAS and we will describe co-added and enhanced resolution (HIRES) maps of the region obtained from IPAC. In addition, the Sh170 molecular cloud has been observed in the $^{12}$CO galactic plane survey of the Five Colleges Radio Observatory (Heyer et al. 1998). These observations are of higher angular resolution than our MWO observations and are useful for comparison with the HIRES map.

[1] A subset of these observations, relating to IRAS 23545+6508, and unrelated to Sh170, has been published elsewhere by Dewdney et al. (1991).

**Table 1.** Parameters for 1420 MHz continuum and HI-line observations.

| | |
|---|---|
| Field centre (J2000) | $00^h01^m33.9^s$ 64°37′42″ |
| Dates of observation | 1986 Oct.–Nov. |
| Interferometer spacings | 12.9 m–617.1 m |
| Synthesized beam (*FWHM*) | 60″ (EW) × 67″ (NS) |
| Continuum calibrators | 3C 147 (21.29 Jy) |
| | 3C 309.1 (7.73 Jy) |
| HI-line calibrator | S7 (100 K) |
| Number of spectral channels | 127 |
| Spectral resolution | 1.32 km s$^{-1}$ |
| Velocity coverage (LSR) | –91.9 to +11.9 km s$^{-1}$ |

## 2. Observations

### 2.1. 1420-MHz continuum emission

Simultaneous observations of the continuum emission and the HI-line emission at 1420 MHz were made in 1986 with the DRAO four-element synthesis telescope (Roger et al. 1973; Landecker et al. 2000). Table 1 contains a summary of the main parameters relevant to these observations.

The continuum emission in a 20-MHz band centred on the HI-line frequency was mapped within the 2°-diameter primary beam of the synthesis telescope. Notch filters excluded HI emission over the central 5 MHz to leave a net continuum bandwidth of 15 MHz. The map was CLEANed with a combination of the Clark (1980) algorithm for the intense point sources and the algorithm of Steer et al. (1984) for the fainter sources and extended emission.

The continuum emission in the central 1° field, corrected for the attenuation of the primary polar diagram, is shown in Fig. 2. This thermal emission from Sh170 shows a close correspondence with the optical nebula (cf. Fig. 1) and includes the central depression adjacent to the position of the exciting star. There are numerous point sources in the field, most of which are almost certainly extragalactic. Note that one such point source lies within the emission from Sh170, approximately 6′ north of the exciting star.

### 2.2. $\lambda$21-cm HI-line emission

The HI emission was mapped in 128 radial velocity channels using a digital cross-correlation spectrometer. Since Galactic HI emission contains structure of all spatial frequencies, observations were made with complete sampling of the $u - v$ plane for east-west baselines from 61$\lambda$ to 2920$\lambda$ at intervals of 20.3$\lambda$. The out-of-band continuum emission, described in the last section, was subtracted from each channel map. Visibilities in the HI line corresponding to baselines less than 61$\lambda$ (i.e. broad structure) were extracted from maps using observations with the DRAO 26-m paraboloid using an identical spectrometer. This single-dish system employed frequency switching to remove instrumental effects and continuum emission. The low and high resolution HI maps were then transformed to the $u - v$ plane, filtered in a complementary manner, and merged

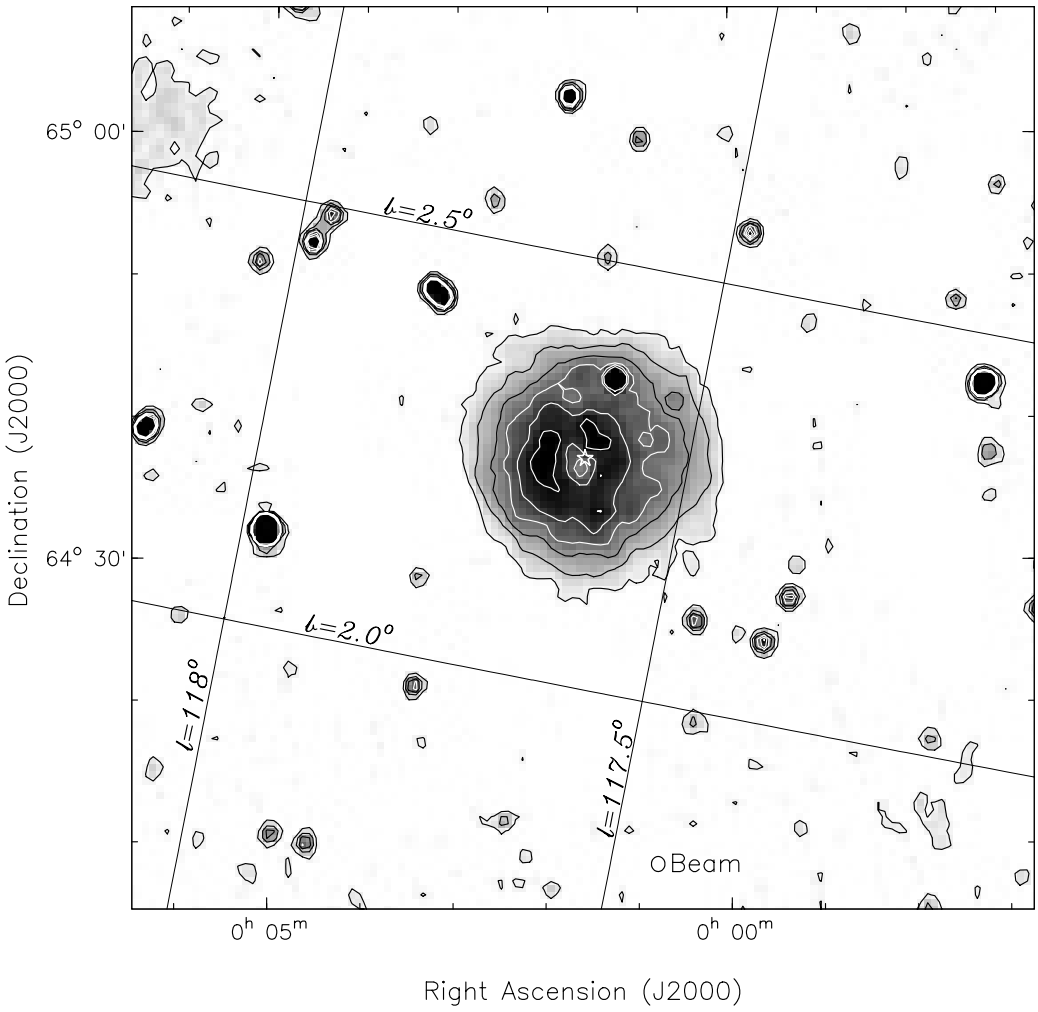


**Fig. 2.** A contoured grey-scale depiction of the continuum emission at 1420 MHz from a 1° field centred on Sh170. Contours (in black) are at 2, 6, and 10 mJy/beam and (in white) at 14, 18 and 22 mJy/beam. The position of the exciting star is denoted with a ⋆ symbol.

to provide 128 maps containing all spatial frequencies up to ∼2900$\lambda$. The HI maps were not CLEANed since the dynamic range of the emission is limited and, with full $u - v$ plane coverage, the low sidelobe level (less than 4%) is such that little would be gained by CLEANing.

Figure 3 shows eight channel-averaged greyscale maps of the HI emission within the 2° field, corrected for primary beam attenuation. These maps cover the velocity sub-range, with respect to the local standard of rest (LSR), −34 to −54 km s$^{-1}$, which includes all HI emission which appears plausibly related to Sh170. This sub-range is indicated in Fig. 4 which is a plot of the total mean spectrum of galactic HI emission in the direction of the HII region as observed with the 35′ beam of the DRAO 26-m telescope (Higgs & Tapping 2000). The maps of Fig. 3 are displayed with the mean level subtracted in order to use the full range of the grey-scale to depict the detailed structure of the atomic hydrogen. One low-level contour of the thermal continuum emission from Sh170 is superposed on the HI images.

In the approximate range −40 to −50 km s$^{-1}$ there is HI emission which is clearly associated with Sh170 and much of this can be seen to effectively surround the ionized nebula. This apparently associated material extends to an angular radius of ∼15′, some 6′ beyond the outer radius of the thermal emission. At many velocities, however, there are areas where it is difficult to discern boundaries between associated HI emission and unrelated features of the atomic component. For example, at velocities −42.5 km s$^{-1}$ and −45 km s$^{-1}$ emission extends to the west and south-west blending with other features in these directions. Similarly, at −45 km s$^{-1}$ and −47.5 km s$^{-1}$ the "surrounding" emission connects to a broad column of emission extending to the north-north-east.

In Fig. 5 we show a map of the HI emission integrated over the velocity range −35.5 km s$^{-1}$ to −52.8 km s$^{-1}$ for which emission appears to be associated with Sh170.

Superimposed on the map is an ellipse which, for the various velocity channels, encompasses most of the associated HI. This boundary crosses the two "bridges" of emission, one of which extends slightly east of north and the other which connects associated emission to the more distributed emission to the west. We will use this ellipse to define the maximum extent of the HI emission related to the Sh170 complex.

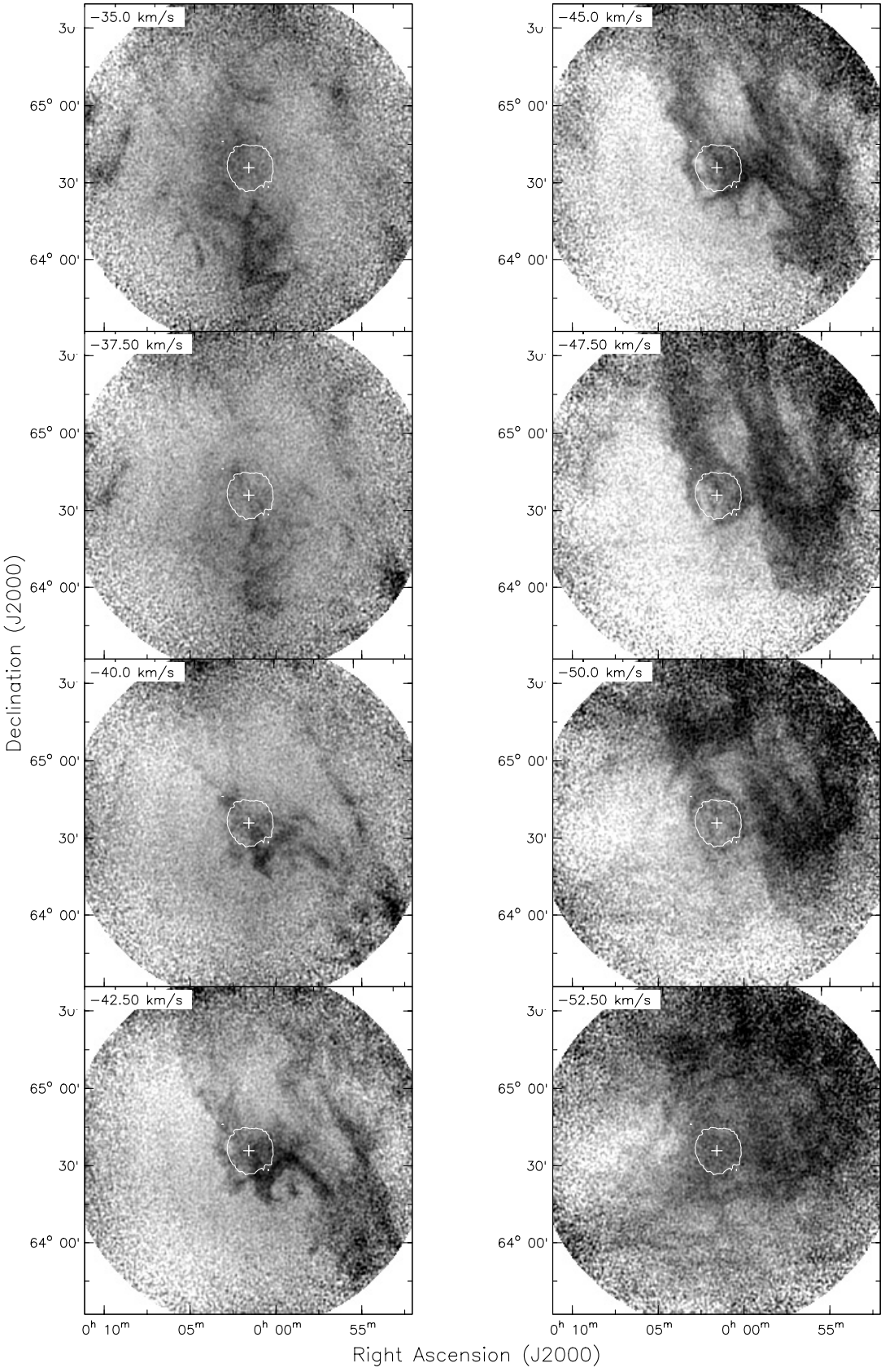


**Fig. 3.** Grey-scale maps of the HI-line emission for 3-channel averages at the indicated radial velocities (LSR). The range white to black represents −30 K to +30 K with respect to the mean level which has been subtracted from each map. An outline of the HII region is shown as a white contour at the 3 mJy/beam level of 1420 MHz continuum emission. The position of the exciting star is shown by a + symbol.

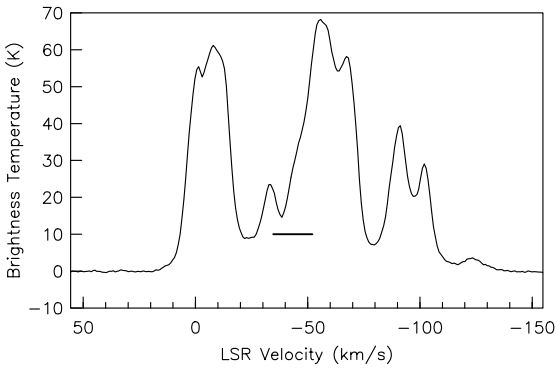


**Fig. 4.** The Galactic HI-line spectrum in the direction of Sh170 as observed with the DRAO 26-m paraboloid (*FWHM* 35′) and corrected for stray radiation (Higgs & Tapping 2000). A horizontal line indicates the radial velocity range for the emission associated with Sh170, as shown in Fig. 3.

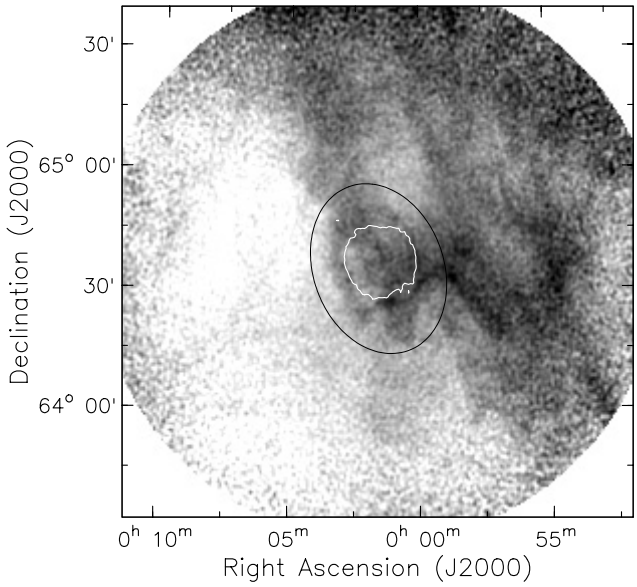


**Fig. 5.** The HI-line emission averaged over the velocity range −35.5 to −52.8 km s$^{-1}$, shown in Fig. 3. The grey-scale represents the range −18 K (white) to +18 K (black) relative to the mean level. The white contour shows the 3 mJy/beam level of the 1420 MHz continuum emission. The ellipse defines the base level for enclosed HI emission assumed to be associated with the Sh170 complex.

### 2.3. Emission of $^{12}$CO and $^{13}$CO, J 1→0

We have mapped an area centred on Sh170 with the 4.9-m telescope of the Millimeter Wave Observatory (MWO) of the University of Texas[2] in the $J$ 1→0 emission of $^{12}$CO and $^{13}$CO with a beamwidth (*FWHM*) of 2.3′. The region of the CO cloud was fully sampled in the observations which were from two observing sessions in 1986 and 1987. A total of 128 spectral channels span a range in radial velocity (LSR) from −54 to −33 km s$^{-1}$, with a channel resolution of 0.163 km s$^{-1}$.

[2] The Millimeter Wave Observatory was operated by the Electrical Engineering Research Laboratory of The University of Texas at Austin with support from the National Science Foundation and McDonald Observatory.

Figure 6 shows the emission of both isomers in 24 channel maps covering the range in radial velocity from −42 to −48 km s$^{-1}$ for which emission can be detected. In projection the cloud subtends only about one-eighth the area of the HII region, and is situated mainly in the quadrant from the north to the west of the exciting star. The $^{12}$CO emission shows two maxima separated by ∼2′ in the north-south direction. The southern peak dominates at velocities more positive than −46 km s$^{-1}$ and the northern peak is predominant at more negative velocities. Despite longer integration times the $^{13}$CO emission was detected over a less extensive area and shows a single maximum coinciding with the southern peak in $^{12}$CO emission with an extension to the more northerly peak. These features can also be seen in Fig. 7 which shows contours of integrated emission in both isomers superposed on a greyscale image of the thermal continuum emission.

$^{12}$CO ($J$ 1→0) emission from this region has subsequently been mapped in the Five Colleges $^{12}$CO Survey of the Outer Galaxy (Heyer et al. 1998). This survey has less spectral resolution than our MWO observations but has superior angular resolution (45″, slightly undersampled) and is thus able to show the spectrally integrated emission in more detail. We use the integrated emission from this survey, recalibrated by Brunt & Ontkean (2003) for the Canadian Galactic Plane Survey (Taylor et al. 2003), to compare with high-resolution images at 100 $\mu$m.

### 2.4. Emission in the far-infrared

Far-infrared emissions in four wavebands centred at 12, 25, 60 and 100 $\mu$m were observed with the IRAS satellite. We have used the co-added images from the various satellite passes, the convolved matched-resolution images of the Infrared Sky Survey Atlas (ISSA), and the derived high-resolution (HIRES) images, all from the Infrared Processing and Analysis Center (IPAC)[3].

Co-added images for the four bands are shown in Fig. 8 superposed on a greyscale depiction of the continuum emission. It can be seen that the emission extends beyond the ionized gas and peaks ∼2′ northwest of the position of the exciting star, as does the peak of the CO emission. The IR emission comprises both an extended cloud and a compact component which is particularly apparent in the 12 $\mu$m image.

The HIRES image at 100 $\mu$m is shown in Fig. 9 superposed as contours on an grey-scale image of the integrated HI emission. This figure clearly illustrates how well the periphery of the extended far-IR emission traces the outline of the atomic gas. Note that there is no distinct HI feature coinciding with the central compact IR emission.

In Fig. 10 we illustrate the central part of the HIRES 100 $\mu$m image, showing the compact component, with contours of the integrated FCRAO $^{12}$CO emission superposed. The CO and compact far-IR components are clearly related and the peaks of the two emissions, while not coincident, are both about 2′ to the north-east of the position of the exciting star.

[3] IPAC is funded by NASA as part of the IRAS extended mission program under contract to JPL.

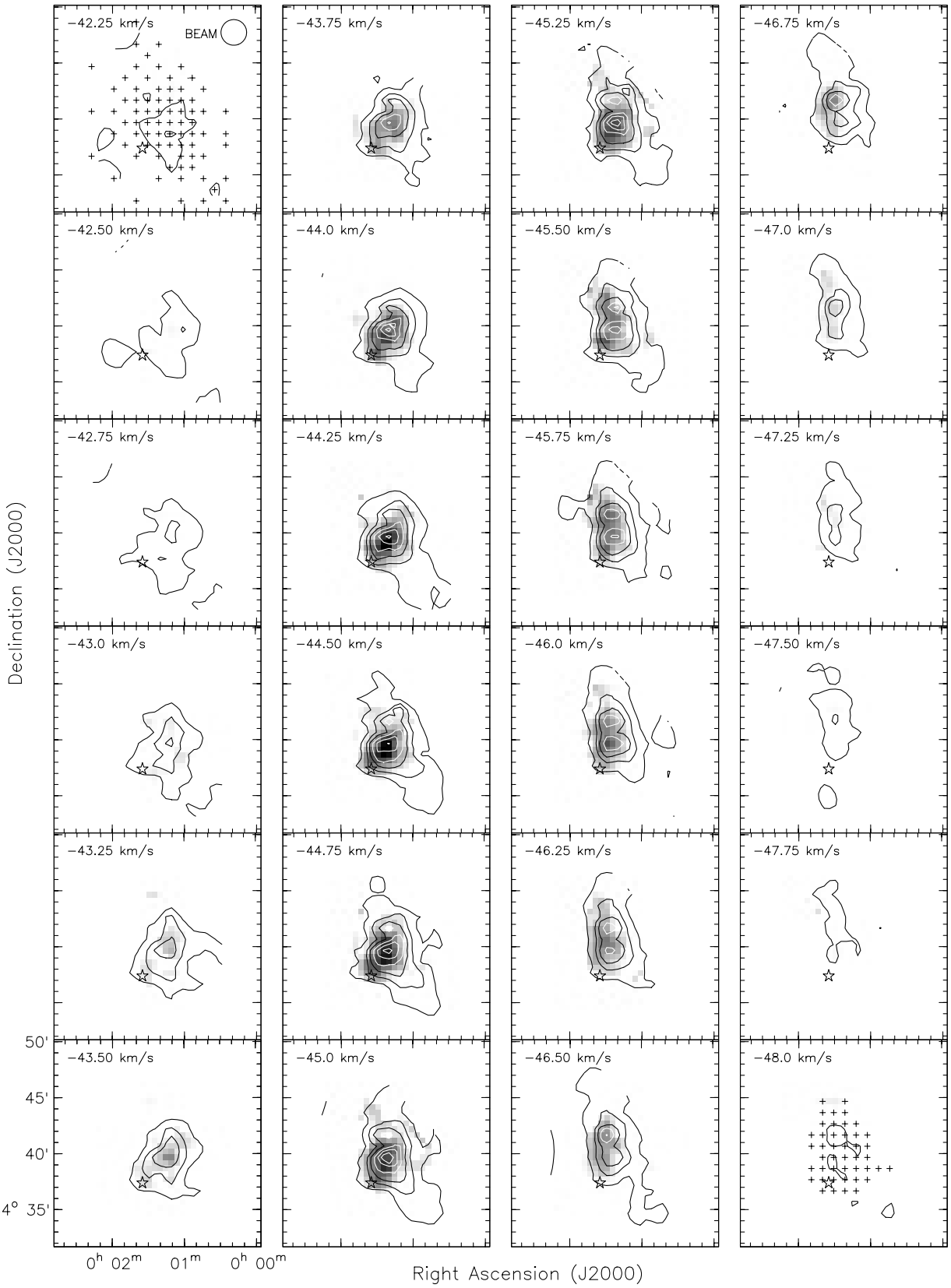


**Fig. 6.** CO emission from the direction of Sh170 for 24 radial velocities as indicated on each map. Emission from $^{12}$CO is indicated by contours (in black) at 1 K, 4 K and 7 K and (in white) at 10 K, 13 K and 16 K. Emission from $^{13}$CO is shown as a grey scale from white (0 K) to black (3 K). The sampling grids for the maps are shown as crosses in the upper-left ($^{12}$CO) and the lower-right ($^{13}$CO) maps. The position of the exciting star is indicated by a ⋆ symbol.

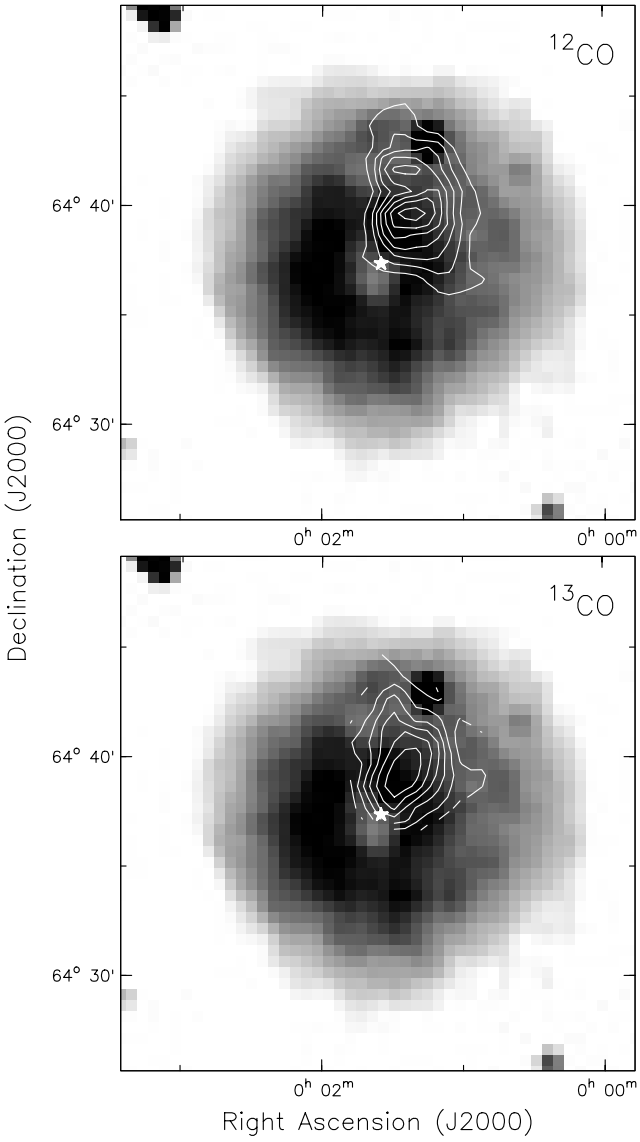


**Fig. 7.** Maps of the integrated $^{12}$CO and $^{13}$CO emission superposed on a grey-scale image of the 1420 MHz continuum emission in the range 0 K (white) to 22 K (black). Contours for $^{12}$CO are at 7 K km s$^{-1}$ intervals to 49 K km s$^{-1}$ and for $^{13}$CO at 1 K km s$^{-1}$ intervals to 7 K km s$^{-1}$. The position of the exciting star is shown with a white ⋆ symbol.

## 3. Gas and dust in association with Sh170

We have calculated a number of physical parameters from the various observations of Sh170, assuming a distance to the complex of 2.2 kpc. Table 2 contains a summary of the values together with the dependence of these on this distance assumption. All masses given in the text and in the table include an assumed helium fraction, $Y = 0.1$.

### 3.1. The ionized gas

We have integrated the thermal emission of Sh170 in the 1.4-GHz continuum map to determine a total flux density for the nebula of 2.5 ± 0.1 Jy. The emission is almost circularly symmetric, with peak brightness temperatures near 3.6 K. For an assumed mean electron temperature of

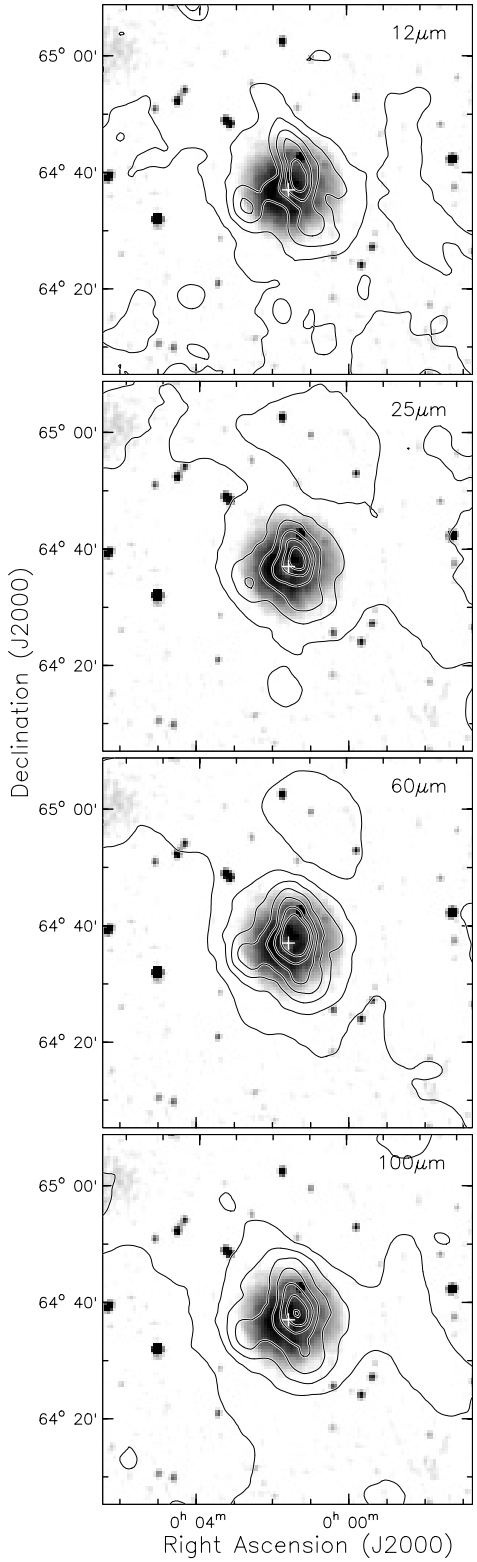


**Fig. 8.** Co-added maps of the far-infrared emission in four bands observed with the IRAS telescope, with the 1420 MHz continuum emission as a background grey scale. Contours are at intervals of 1 MJy/sr (12 $\mu$m), 2 MJy/sr (25 $\mu$m), 10 MJy/sr (60 $\mu$m) and 25 MJy/sr (100 $\mu$m). The star position is shown with a + symbol.

8000 K, this corresponds to a peak emission measure of 2150 nucleons$^2$ cm$^{-6}$ pc. There is a small central depression of diameter ∼3 ′ or ∼2 pc at the assumed distance of 2.2 kpc,

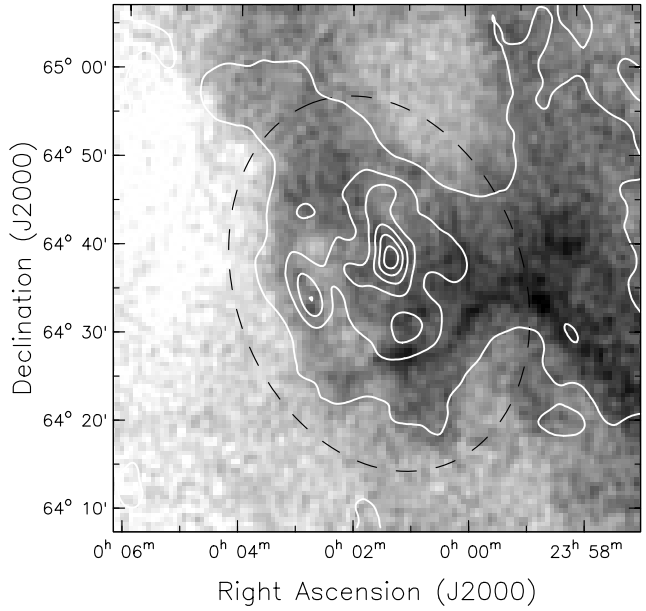


**Fig. 9.** Contours of the 100 $\mu$m HIRES image superposed on the HI-line emission averaged over the velocity range −35.0 to −52.8 km s$^{-1}$, shown as a grey-scale. The range in HI emission is from −18 K (white) to +18 K (black) relative to the mean level. Far-infrared contours are at intervals of 50 MJy/sr. The dashed line indicates the ellipse shown in Fig. 5.

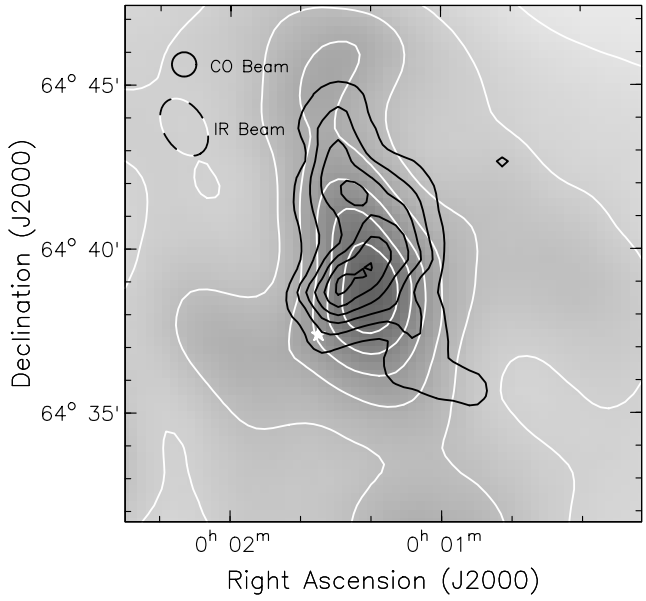


**Fig. 10.** The 100 $\mu$m HIRES map toward Sh170 as a grey-scale with (white) contours at intervals of 40 MJy/sr, and the integrated $^{12}$CO emission superposed in (black) contours at intervals of 7 K km s$^{-1}$. The star is at the position marked with a ⋆ symbol.

with the emission measure at the centre decreasing to approximately half the surrounding values.

If all the ionizing photons from the exciting star were captured by the nearby surrounding gas, the measured flux density together with an assumed distance would provide an estimate of the excitation parameter of the star, using the relations derived by Schraml & Mezger (1969). For a flux density of 2.5 Jy and a distance of 2.2 kpc, we estimate a value, $U$ = 30.1 pc cm$^{-2}$, close to the value of 30.5 pc cm$^{-2}$ for an O9.5V star given by Panagia (1973) and equivalent to the log number of ionizing photons per second of log $N_L$ = 48.1. This value can be compared to two more recent calculations of the numbers of ionizing photons for early main sequence stars which indicate an effective stellar temperature near 33 kK (Vacca et al. 1996) or near 35 kK (Diaz-Miller et al. 1998), implying a spectral type in the range O9.5V - B0V. However, considering that the optical morphology suggests that much of the ionization is density-limited, we must treat our measured value as a lower limit to the true excitation of the star.

**Table 2.** Summary of measured and derived parameters of various components of Sh170 for $d_{2.2}$ = distance/2.2 kpc. Densities are given as nucleons per volume and nucleons per column area.

| | |
|---|---|
| **Ionized component** | |
| flux density (1420 MHz) | 2.5 ± 0.1 Jy |
| peak brightness | 4.3 K |
| maximum diameter | 14($d_{2.2}$) pc |
| excitation parameter | 30.1 ± 1.0 $(d_{2.2})^{2/3}$ pc cm$^{-2}$ |
| mass | 350 ± 100 $(d_{2.2})^{2.5}$ $M_\odot$ |
| mean density | 16 ± 7 $(d_{2.2})^{-1/2}$ cm$^{-3}$ |
| central emission measure | 2150 cm$^{-6}$ pc |
| central column density | 2.9 × 10$^{20}$ $(d_{2.2})^{1/2}$ cm$^{-2}$ |
| central cavity diameter | 2 $(d_{2.2})$ pc |
| displaced mass | 7 ± 2 $(d_{2.2})^{2.5}$ $M_\odot$ |
| mean radial velocity | –50 km s$^{-1}$ |
| **Atomic component** | |
| associated mass | 910 ± 90 $(d_{2.2})^2$ $M_\odot$ |
| mean density | 9 ± 2 $(d_{2.2})^{-1}$ cm$^{-3}$ |
| typical column density | 5 × 10$^{20}$ cm$^{-2}$ |
| mean radial extent | 10 $(d_{2.2})$ pc |
| mean radial velocity | –45.0 km s$^{-1}$ |
| **CO-related component** | |
| total mass | 1150 ± 250 $(d_{2.2})^2$ $M_\odot$ |
| peak column density | 2.3 ± 0.5 ×10$^{22}$ cm$^{-2}$ |
| mean density | 1900 $(d_{2.2})^{-1}$ cm$^{-3}$ |
| overall extent | 5.5 $(d_{2.2})$ pc × 3.5 $(d_{2.2})$ pc |
| mean radial velocity | –45 km s$^{-1}$ |
| **Dust-related parameters** | |
| stellar extinction | $2\overset{m}{.}7 \pm 0\overset{m}{.}2$ |
| column density to star | 5.1 × 10$^{21}$ cm$^{-2}$ |
| infrared flux | 1.03 × 10$^{-10}$ W m$^{-2}$ |
| IR luminosity | 15 500 $(d_{2.2})^2$ $L_\odot$ |
| **Extended IR component** | |
| overall extent | 24 $(d_{2.2})$ pc × 16 $(d_{2.2})$ pc |
| implied dust temperatures | 23 K–31 K |
| **Compact IR component** | |
| overall extent | 7 $(d_{2.2})$ pc × 3.5 $(d_{2.2})$ pc |
| implied dust temperature | 17 K |

The velocity field of the H$\alpha$ emission from Sh170 has been investigated in detail by Miville-Duchênes et al. (1995) using a Fabry-Perot camera. They find that the mean $V_{\rm LSR}$ of the ionized gas is $-50.10 \pm 0.08$ km s$^{-1}$, with a velocity dispersion (standard deviation) of 8.70 km s$^{-1}$, close to typical values for HII regions (Joncas & Roy 1986). A north-south gradient in velocity of $\sim$1.4 km s$^{-1}$ pc$^{-1}$ is detected, with less negative velocities corresponding to the more northerly ionized gas. If we use the mean velocity of the CO emission ($-45.0$ km s$^{-1}$) as a reference or systemic velocity, 80% of the 12,695 measured H$\alpha$ velocities are more negative than this, indicating that the ionized gas is largely streaming toward us. The mean relative velocity for all the ionized gas is $\sim$5 km s$^{-1}$, and the median relative velocity of the "approaching" component is $\sim$7 km s$^{-1}$.

To estimate the mass of ionized gas, we have made use of the circular symmetry of Sh170 and have chosen to model the mean projected radial decline in the thermal continuum emission outward from the centre. We assume an electron temperature of 8000 K, and a hemispheric region, circularly symmetric about the line-of-sight which is confined to the near side of the exciting star. A good fit to the mean radial emission profile is achieved in a model with a density profile declining from a central value of 21 ions cm$^{-3}$ to zero at an outer radius of 7 pc. This fit gives a volume weighted mean density of 13 ions cm$^{-3}$ and a total mass of 320 $M_\odot$. The emission can also be modelled, less realistically, by assuming a full spherically symmetric region with density declining from a central value of 15 ions cm$^{-3}$ to zero at an outer radius of 7 pc. The total mass of ionized gas would then be 450 $M_\odot$. As a third model we consider a cylindrical slab, 4 pc constant depth (along the line-of-sight), with density declining outward along projected radii. For this model we can fit the profile with a total mass of 250 $M_\odot$ and a central density of $\sim$23 atoms cm$^{-3}$. The second and third models are simplistic and are meant only as extremes to bracket an estimate of the probable mass of $350 \pm 100$ $M_\odot$ and an estimate of the mean volume density of $16 \pm 7$ atoms cm$^{-3}$.

We have separately modelled the small central depression in the thermal emission and estimate that the gas displaced to form the depression would have a mass of $\sim 7 \pm 2$ $M_\odot$.

### 3.2. The atomic gas

The maps of Fig. 3 illustrate the difficulty of delineating the boundary between HI which is clearly associated with Sh170, the exciting star and the molecular cloud and HI which is merely part of the nearby interstellar medium. Figure 4 shows the existence of background extended emission with a substantial gradient over the radial velocity range associated with Sh170. This broad emission may or may not be due to diffuse gas at a similar distance to the nebula. However, any diffuse inter-cloud gas which is near the molecular cloud is likely to have been dissociated by the general interstellar radiation prior to the formation of the exciting star. On the other hand, the HI that is clearly associated with the HII region, particularly in the velocity range $-42$ to $-50$ km s$^{-1}$, where the atomic gas surrounds the ionized component, is sufficiently irradiated by the star to remain atomic even in the absence of any external interstellar radiation.

Assuming the HI emission to be optically thin, and a distance to Sh170 of 2.2 kpc, we have integrated the HI emission within the ellipse of Fig. 5 to calculate a total mass of atomic gas of $1000 \pm 70$ $M_\odot$. The levels used in the integration are those above a base level fitted to the emission at the ellipse, avoiding the "bridge" regions on the north and west of the area. Averaging over the area within the ellipse yields a volume-weighted mean HI density of $9 \pm 2$ atoms cm$^{-3}$, and a mean atomic column density of $5 \times 10^{20}$ atoms cm$^{-2}$. It can be argued that the ellipse and/or the velocity range of the integration in Fig. 5 ($-35.5$ to $-52.8$ km s$^{-1}$) includes HI emission that may not be associated with, or affected by Sh170 and the exciting star. Hence, we have also integrated the emission within a quasi-circular polygon closely surrounding Sh170 and the peripheral HI, of mean radius 15.6′, and over a more restricted range in velocity ($-39$ to $-51$ km s$^{-1}$). From this integration, we derive a total HI mass of $820 \pm 60$ $M_\odot$. We will use the mean of these two mass calculations, $910 \pm 90$ $M_\odot$, as our best estimate for the associated atomic component.

There are numerous compact features in the 3-channel averages of Fig. 3 with widths of typical size of $\sim$3 pc, and with column densities in the range of $1$–$2 \times 10^{20}$ atoms cm$^{-2}$. With depths assumed equal to projected widths, these features would have densities in the range 10 to 20 atoms cm$^{-3}$.

### 3.3. The dense molecular gas

Figure 7 illustrates the relatively compact CO cloud associated with Sh170. The integrated $^{12}$CO emission is confined within an area $5.5' \times 9'$ or $3.5 \times 5.5$ pc$^2$ at a distance of 2.2 kpc. For comparison, the $^{13}$CO emission is detected within a somewhat smaller area $4.5' \times 7'$ or $3 \times 4.5$ pc$^2$. Kutner & Leung (1985) have studied in detail the conversions of CO intensities to molecular hydrogen masses and the dependance of these on relative CO abundance and cloud kinetic temperatures. We will use their models and separately established relationships to estimate the total gas densities and masses of the cloud as inferred from emissions of the two isomers.

First, we employ the relations of Sanders et al. (1984) based upon the measured correlation of $^{13}$CO integrated intensities with extinction in dark clouds and the gas-to-dust ratio of Bohlin et al. (1978). These relations make no assumptions regarding LTE in the measured clouds and yield a column density of molecular hydrogen in terms of integrated emission $(2.1 \pm 0.5) \times 10^{21}$ molecules cm$^{-2}$ (K km s$^{-1}$)$^{-1}$. Because of the proximity of the O9V star the excitation of the CO is likely to be somewhat greater than for isolated dark clouds. The models of Kutner & Leung confirm this, and, for a kinetic temperature of 17 K (estimated from the peak $^{12}$CO temperatures) and an abundance $Q = [{\rm CO}]/[{\rm H_2}] = 5 \times 10^{-5}$, yield a conversion ratio of $1.4 \times 10^{21}$ molecules cm$^{-2}$ (K km s$^{-1}$)$^{-1}$. From this we calculate a peak total gas column density from the $^{13}$CO emission of $1.9 \pm 0.7 \times 10^{22}$ nucleons cm$^{-2}$, and an integrated total cloud mass of 900 $M_\odot$.

For the cloud as represented by the $^{12}$CO emission, we use the work of Digel et al. (1996) which relates the column density of molecular hydrogen to the integrated intensity of $^{12}$CO emission using the high-energy gamma-ray emission from molecular clouds in the Perseus arm, measured with the EGRET instrument of the Compton Observatory, as an independent tracer of mass. The ratio of molecular column density to integrated emission inferred from this study is $(2.5 \pm 0.9) \times 10^{20}$ molecules cm$^{-2}$ (K km s$^{-1}$)$^{-1}$. This value is very close to the $^{12}$CO conversion ratio of Kutner & Leung for a kinetic temperature of 17 K, a mean density of 1500 molecules cm$^{-3}$ and $Q = 5 \times 10^{-5}$. With this relation we find that the peak total gas column density for the $^{12}$CO cloud is $(2.7 \pm 1.0) \times 10^{22}$ nucleons cm$^{-2}$ and the integrated total cloud mass is 1400 $M_\odot$.

The rough agreement between the estimates for the two isomers of CO may be partly accidental. At first sight, one might expect higher values for the $^{13}$CO integrations, given that this emission should be less affected than $^{12}$CO emission by substantial optical depths in the lines. However, any such effect may be offset by the greater extent of the detected $^{12}$CO cloud, both in angle and in radial velocity, possibly in some part due to a higher dissociation rate for $^{13}$CO in the high uv environment (e.g. Warin et al. 1996).

We will use the mean of the $^{12}$CO and $^{13}$CO values of total gas column density and mass for estimates of other related parameters. A mean volume density in the molecular cloud can be estimated from the peak central column density and an estimate of the total depth through the cloud. If we assume a cloud depth equal to a mean projected width, ~3.9 pc, and the mean peak column density, $2.3 \times 10^{22}$ nucleons cm$^{-2}$, we estimate a mean volume density of ~1900 nucleons cm$^{-3}$. Note that this value is some two orders-of-magnitude higher than estimated densities in the atomic and ionized components of the Sh170 complex.

### 3.4. The dust components

From the 100 $\mu$m HIRES image of Fig. 9 we can distinguish the following components of dust emission: (i) a relatively compact component which is associated with the CO cloud as featured in Fig. 10; (ii) extended emission around Sh170, the outline of which follows the HI emission distribution in the range −35 to −53 km s$^{-1}$ out to projected radii of 8–14 pc at various position angles; and (iii) extended emission at larger distances from Sh170, particularly to the west which also correlates with HI emission but is probably unrelated to Sh170. In addition, we dectect no far-infrared component correlated with the HII region itself.

The association of the compact component of 100 $\mu$m emission with the CO cloud ((i) above) is strengthened quantitatively by comparing the mean radial distributions of the far-IR emission and the $^{12}$CO emission observed in the FCRAO survey. In both cases the mean distributions were determined from the areas within various contour levels of the images. Both yield a $1/e$ radius, corrected for beam broadening of 1.′8, corresponding to a mean projected width of 2.3 pc for the cloud at a distance of 2200 pc.

We have integrated the far-IR emission associated with Sh170 (components (i) and (ii) above, but dominated by (ii)) from the co-added images in each of the four IRAS bands (Fig. 8) down to the level of the lowest circumscribing contour in each image. The flux densities, corrected for the DIRBE re-calibration, are 81 Jy, 127 Jy, 917 Jy and 1780 Jy at the wavelengths 12 $\mu$m, 25 $\mu$m, 60 $\mu$m, and 100 $\mu$m respectively. An integration over frequency under a 25 K blackbody curve ($\lambda^{-2}$ emissivity) fitted to the 100 $\mu$m value with a smooth extension to fit the shorter wavelength flux densities yields a total infrared flux of $1.03 \times 10^{-10}$ W m$^{-2}$. (This value is not especially sensitive to the assumed dust temperature, and is almost identical to that obtained by using the integration algorithm of Casoli et al. 1986.) For the presumed distance of 2.2 kpc, the infrared luminosity is $1.55 \times 10^4$ $L_\odot$ ($\log(L/L_\odot) = 4.2$). If all the uv photons emitted by an O9V star at this distance were ultimately absorbed by the nearby surrounding dust and contributed to its heating, we would expect to detect a greater IR luminosity by a factor of ~5. This indicates that less than 20% of the photons from the exciting star of Sh170 are actually captured by the dust in close proximity.

At first glance the distributions of the extended emissions are rather similar in the four IRAS bands with the peak of emission displaced from the position of the star toward the peak of high-density gas as revealed by the CO emission. However, a map of the ratio of the 60 $\mu$m and 100 $\mu$m emissions from the IRAS Sky Survey Atlas (ISSA), both convolved to the same resolution and corrected for background emission, shows that this colour index ratio peaks at the position of the exciting star and declines monotonically outwards with close to circular symmetry. Because of the low resolution of the ISSA maps, the extended component ((ii) above) is dominant in the ratio map. We will use contours of this ratio in the next section.

## 4. The inter-relation of the various components

### 4.1. Diffuse gas and dust

We find no dust emission corresponding to the ionized component of Sh170. By contrast, we have identified co-extensive components of emission from HI and dust out to radii of ~12 pc from the exciting star. However, Fig. 9 shows that, although the atomic component has a remarkably similar boundary to that of the dust emission (component (ii)), there is not a strong detailed correlation of the two emissions.

The radial decline of the ratio of the matched-resolution emissions at 60 $\mu$m and 100 $\mu$m almost certainly reflects a decline in dust temperature outward from the star. However, because a substantial but unknown proportion of the emission at 60 $\mu$m is from non-equilibrium radiation of very small grains, this ratio of the emissions at any radius is not expected to yield a reliable estimate of dust temperature. Instead, we choose to compare the average radial profiles of the 100 $\mu$m emission and the HI column density in the following manner to derive dust temperatures (cf. Roger 2002).

Boulanger et al. (1996) have correlated the far-infrared emission from dust measured with the DIRBE and FIRES experiments of the Cosmic Background Explorer (COBE)

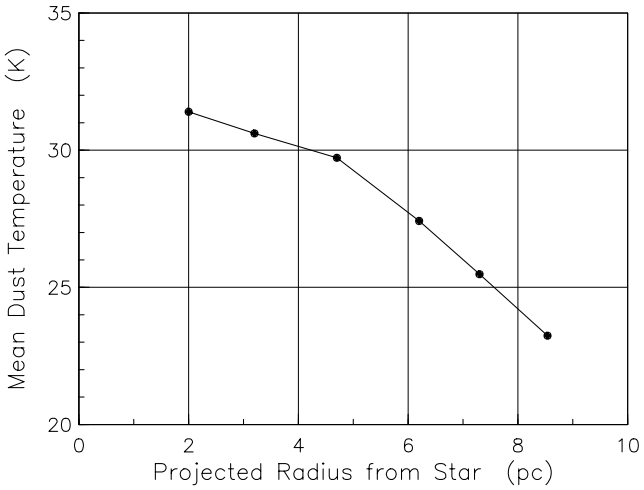


**Fig. 11.** The variation of mean dust temperature as a function of projected radius from the exciting star, derived from the ratio of HI column densities and IRAS 100 $\mu$m intensities using Eq. (1).

with HI at high latitudes observed in the Leiden/Dwingeloo Survey (Hartmann & Burton 1997). They find that for $\lambda$ 100 $\mu$m to 1 mm, the data are well fit by a Planck curve with $T$ = 17.5 K, emissivity proportional to $\lambda^{-2}$ and $I_{100}$ = 0.54 MJy sr$^{-1}$/10$^{20}$ nucleons cm$^{-2}$. Because of the known calibration difference between COBE and IRAS data, the appropriate relation for IRAS data is $I_{100}$ = 0.85 MJy sr$^{-1}$/10$^{20}$ nucleons cm$^{-2}$ for regions of column density less than 5 $\times$ 10$^{20}$ nucleons cm$^{-2}$ (Boulanger et al. 1999). The relation is in close accord with the dust model of Draine & Lee (1984) for compact graphite and silicate grains and can be used for an indirect measure of dust temperature in situations where we can assume a similar mix of dust and gas to that in the high latitude studies cited above. Since for $\lambda \geq 100\,\mu$m the black body emission of dust at temperature $T_{\rm d}$, $I_\nu \propto [\exp(h\nu/kT_{\rm d}) - 1]^{-1}$ we can use the above emissions ratio measured for dust at 17.5 K to derive the dust temperature for other values of IRAS emission at 100 $\mu$m, $I_{100}$, and column densities, $N_{\rm H}$ nucleons cm$^{-2}$:

$$T_{\rm d} = 143.9/\log_{\rm e}\left[3.16\times10^{-17}\,(N_{\rm H}/I_{100}) + 1\right]\ \text{K}. \qquad (1)$$

To derive the dust temperature profile with this equation, we have averaged the 100 $\mu$m emission from the HIRES map and the column densities from the integrated HI map along the quasi-circular arcs of the contours of the $I_{60}/I_{100}$ colour ratio (cf. Sect. 3.4). In calculating the averages we have avoided the areas in the northwest quadrant which contain emission from the CO cloud and compact IR component. Figure 11 shows the radial decline of dust temperature derived in this way, varying from 31.3 K at 3.1′ (~2 pc) from the star to 23.2 K at 13.3′ (~8.5 pc). It is important to note that we have used emissions at *projected* radii, averaged along the lines-of-sight. Even considering the fact that the IR emission is a strong function of temperature and hence warmer regions will be weighted excessively in any such average, the dust temperatures at inner distances from the star are almost certainly higher than is shown in Fig. 11. We note also that, beyond a radius of ~15′, the variations in the general background level of integrated HI are such as to preclude reliable estimates of mean dust temperature.

### 4.2. Dense gas and dust

We have remarked on the close relationship of the CO cloud with the IR (HIRES) compact component apparent in Fig. 10. We can use the implied peak gas column density (2.3 $\times$ 10$^{22}$ nucleons cm$^{-2}$) derived from the FCRAO map with the relationship of Digel (1996) (cf. Sect. 3.3) and the peak 100 $\mu$m intensity of the compact dust component (~200 MJy sr$^{-1}$) in Eq. (1) to derive a mean dust temperature at this position. The value, 17.7 K, is somewhat in excess of the peak temperature in the individual $^{12}$CO channel maps of 14.9 K. Although one might expect the gas and dust temperatures in the dense cloud to be similar, we note that the two observations will weight the gas and dust in the cloud in very different ways.

It is of some interest to know whether or not the measured and estimated parameters for the molecular cloud are consistent with it being gravitationally bound. In a simple view, we would expect a cloud of mass $M$ = 1150 $M_\odot$ (Table 2) confined within a mean radius $r$ = 1.4 pc (deduced from the areas of the contours of integrated CO emission) to be bound if the mean random velocity $v < \sqrt{6GM/5r}$ or 2.1 km s$^{-1}$. From an inspection of the data of the MWO observations we find that the line widths of the CO emission, which reflect thermal and turbulent motions, indicate that this condition is satisfied. A more thorough treatment of the energy balance would require observations of higher resolution and a consideration of the possible effects of magnetic fields and external pressures on the molecular cloud.

### 4.3. Stellar extinction and column densities

Measurements of colour indices for the exciting star (Mayer & Macák 1973 and others) indicate a value of $E_{B-V}$ near 0.86$^{\rm m}$, which implies a visual extinction of ~2.75$^{\rm m}$. Assuming standard calibrated reddening-to-gas ratios (Bohlin et al. 1978) we would expect a total gas column density to the star of (5.1 $\pm$ 1.5) $\times$ 10$^{21}$ nucleons cm$^{-2}$ and a HI column density of (4.1 $\pm$ 1.2) $\times$ 10$^{21}$ atoms cm$^{-2}$. We can compare these values with an integration of the HI emission from the local gas velocities to the systemic velocity of the region as determined from the atomic and molecular emissions.

We have integrated the HI emission averaged over a 1.5′-diameter region centred on the star over the range +15 km s$^{-1}$ to −45 km s$^{-1}$. The integration yields a HI column density to Sh170 of 3.3 $\times$ 10$^{21}$ atoms cm$^{-2}$, within the range of that implied by the obscuration. An integration over the same velocity range of the spectrum shown in Fig. 4 of a 36′-diameter area, gives a similar column density of 3.0 $\times$ 10$^{21}$ atoms cm$^{-2}$, indicating that the value in the smaller area centred on the star is typical of that for the larger area. Expanding the integration limit to include HI emission to −50 km s$^{-1}$, the extreme of any plausible systemic velocity, increases the column density in the 1.5′ diameter region to 3.7 $\times$ 10$^{21}$ atoms cm$^{-2}$. The agreement between the measured column density and that deduced from the measured $E_{B-V}$ is well within the scatter of values determining the ratios of Bohlin et al. (1978).

It is clear that the HII region is largely on the near-side of the overall complex, as indicated by the lack of any obscuration

resembling the shape of the dense molecular cloud (cf. Figs. 1 and 7), and by the relative mean radial velocities of the components. Specifically, the ionized gas from H$\alpha$ measurements has an average approach velocity relative to the systemic velocity of $\sim$5 km s$^{-1}$. Our estimated column density through this ionized gas is approximately $3 \times 10^{20}$ nucleons cm$^{-2}$. Although we find no component of far-infrared dust emission corresponding to the ionized gas, we note that Fig. 1 does show a few patches of obscuration which may be small clumps of high density gas and dust embedded within the diffuse ionized medium.

From the FCRAO map of $^{12}$CO and the conversion relation of Digel et al. 1996 we can estimate the dense compact cloud gas column density at the position of the star to be $\sim 7 \times 10^{21}$ nucleons cm$^{-2}$, a value approximately one-third the estimated column density through the CO cloud at its centre. Since a dust component expected from this column density would produce an additional visual extinction of $\sim 4.5^{\rm m}$ (which is not seen), it is reasonable to conclude that the entire molecular cloud is on the far side of the star.

### 4.4. The distance from the star to the molecular cloud

The observed CO cloud in the direction of Sh170 is isolated and in a region of the outer Galaxy which is relatively sparse in molecular clouds. The exciting star and the other stars in the small open cluster would each have formed from a dense concentration comprising only a fraction of the total parent cloud material, leaving the remainder as a remnant cloud. We consider it likely that the observed cloud is this remnant of the cloud from which the exciting star formed; otherwise we would have to postulate a second cloud, no longer detectable, as the parent cloud, lying coincidentally along the line-of-sight to the observed CO cloud.

We have noted that the star is on the near side of the molecular cloud and that the projected offset of the star from the peak of the CO cloud is 2′ or 1.3 pc at the presumed distance of 2.2 kpc. The component of separation along the line-of-sight may be more or less than this amount. However, the greater the presumed separation, the more coincidental is the close alignment of the star-cloud direction with the line-of-sight. For this reason, we suggest that the simplest assumption is that the total distance from the star to the cloud is not greatly in excess of the projected separation of the star from the CO emission peak. We will favour this assumption in our subsequent discussion while allowing some credence to the possibility of a larger separation.

## 5. Discussion

### 5.1. Development of the HII region

Our observations are consistent with the interpretation of Sh170 having developed as a "blister" HII region (Israel 1978) within a molecular cloud, of which the small molecular cloud which we now detect is probably a remnant. Although in terms of the lifetime of the exciting star the region may be still relatively young, much of the parent cloud material initially in close proximity will now be ionized and dispersed and a blister description is no longer apt. In their interpretation of the H$\alpha$ emission from Sh170, Miville-Duchênes et al. (1995) concluded that several kinematic and morphological features of this emission are in accord with the "champagne" model proposed by Tenorio-Tagle (1979) to explain such regions. The model describes how the ionization front of an early-type star, embedded near the edge of a dense cloud, breaks out through the cloud boundary and the pressure difference between cloud and inter-cloud gases drives ionized matter out of the cloud with supersonic velocities and an accompanying isothermal shock. Miville-Duchênes et al. find that their measured velocity field gradient is consistent with a small angular offset of the outflow axis from the light-of-sight of $\sim 15°$.

Two-dimensional model calculations (Bodenheimer et al. 1979; Yorke et al. 1982) show that a champagne flow initiated by an O-star near the edge of a dense cloud will produce an extended low-density HII region, through which a large percentage of the ionizing photons can escape. These models further demonstrate that, with such flows, a single O-star is capable of substantially eroding the parent molecular cloud during its lifetime. By scaling the erosion rate for an O7V star in molecular gas of density 600 nucleons cm$^{-3}$ from Yorke et al. to that appropriate to an O9V star in a similar density, we estimate the erosion to amount to $\sim 1.4 \times 10^{-3}$ $M_\odot$/year. If the ionized gas of Sh170 represents the total mass eroded ($\sim$350 $M_\odot$), then we can estimate an age for the region of $2.5 \times 10^5$ years. This age can be combined with the radius of the HII region to provide an estimate of the velocity of the eroded material. An HII radius of 6 pc combined with this age implies a velocity of 24 km s$^{-1}$. While this velocity is within the range expected from champagne model calculations (e.g. case 1 of Bodenheimer et al. 1979), it is somewhat in excess of the streaming velocities measured for Sh170 by Miville-Duchênes et al. (see their Fig. 2) which are mostly in the range $-5$ to $+15$ km s$^{-1}$ with respect to the velocity of the molecular cloud. This suggests that the erosion rate may be closer to half this value (say $7 \times 10^{-4}$ $M_\odot$/year) with an age for the region of $\sim 5 \times 10^5$ years. Note, however, that current champagne models take no account of any dissociated (HI) component in the ablated material.

We favour, then, a picture of Sh170 with radiation from the exciting star ablating material from the molecular cloud, ionizing and accelerating it outward to the intercloud medium, over at least the nearside hemisphere, for a period of several times $10^5$ years. If the star is as close to the molecular cloud along the line-of-sight as it is in the perpendicular dimensions, the HII region is likely still to be photon bounded on the far side with the ionization front continuing to advance into the dense cloud. In a paper considering the limitations on star formation in molecular clouds, Franco et al. (1994) conclude that the most efficient cloud destruction mechanism is through the evaporation of gas by O-stars located near the cloud boundaries. In their view, the thermal pressure of the ionized gas drives the outflow into the intercloud medium and the growth of the of the region inside the cloud is determined primarily by the mass efflux and the attendant drop in absorption of stellar UV radiation between the ionizing star and the ionization front. The formation and evolution of HII regions in the density gradients of

cloud boundaries has been investigated by Franco et al. (1990) who show how, with the appropriate conditions, a conical region of outflowing ionized gas develops, centred about an axis along the direction of maximum decreasing density. We suggest that this describes what is observed for Sh170. The HII region around the O9 star may have begun as a blister within the nearside boundary of the cloud concentration from which it formed but soon broke through as a champagne outflow on the low density side. Through erosion over time, the cone of ionized outflow would have widened but with the star remaining in or near a region of substantial density gradient on the edge of the remaining molecular cloud. In the direction from the star toward increasing density the region would be photon-bounded with the ionization front advancing slowly into the cloud. However, in directions from the star roughly transverse to the line-of-sight where the ionization front would encounter approximately constant density, we would expect the ionization front to advance more rapidly into an annular region outside the cone of the outflow. We propose that this annular region would permit the persistence of a dissociation front in advance of the ionization. The resulting zone of atomic hydrogen is the subject of the third option considered in the next section.

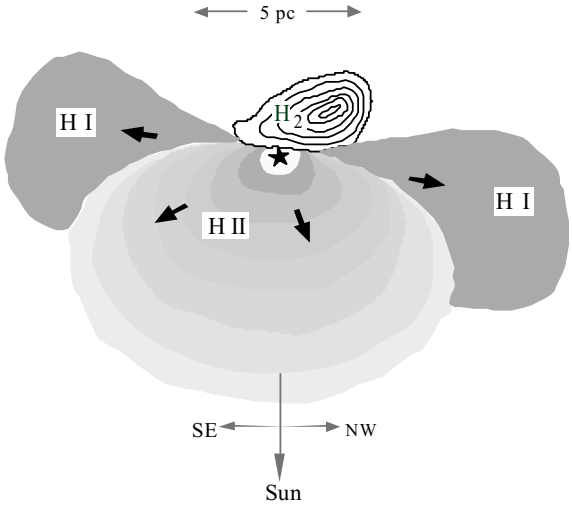


**Fig. 12.** A suggested model cross-section through the components of Sh170 to show their relative positions. The cut is a plane defined by the line-of-sight and a line running approximately SE-NW through the star and the centre of the molecular cloud.

### *5.2. Origin of the HI in the region*

Our picture of the origin and evolution of the atomic hydrogen near Sh170 is less clear. Parts of the emission in the area (e.g. the bridges to the north and west) are clearly connected to the general interstellar HI distribution. On the other hand, much of the HI emission, particularly in the velocity range −40 to −50 km s$^{-1}$, has a boundary which closely mimics, at a larger radius, the circular boundary of the ionized gas. Although the mean line-of-sight velocity of the HI is close to that of the molecular gas, this circular association is somewhat more apparent for emission at velocities more negative than the mean (i.e. approach velocities). Integrated over velocity, the HI emission seems to be related to the extended, heated dust emission in the region with both components centred on the position of the O9V star.

What is the origin of this atomic gas, particularly that within the quasi-circular boundary? We consider three possibilities. First, the gas may be merely part of the pre-existing interstellar distribution in the area from which the molecular cloud and, subsequently, the O-star formed. The HI would have a "normal" dust component subject to heating by radiation from the central star. The circular boundary of much of the HI emission might represent the outer radius to which pre-existing neutral interstellar gas has been displaced and piled up by radiative action of the exciting star or an associated ionization front. Alternatively, it may represent a warm neutral halo surrounding the original (pre-star-formation) molecular cloud as is found near dark clouds (e.g. Andersson et al. 1992). It is significant to note, however, that the circular boundaries of both the HI and the HII are centred on the star, and not on the centre of the molecular cloud.

As a second possibility, the HI may represent a recombined component of gas ionized and expelled in the champagne flow from the molecular cloud. To further consider this idea, we would need to find a reason for recombination to commence so early in the main sequence lifetime of the star. Relative motion of the star toward the cloud centre could facilitate recombination, and it is worth noting that the exciting star is indeed displaced from the centre of the supposed stellar wind cavity in the direction of the cloud centre. However, since the far-infrared emission shows no dust component corresponding to the ionized emission from Sh170, we would need to explain how any newly recombined gas had re-acquired what appears to be a normal dust component in a relatively short time.

Thirdly, the atomic gas may be a dissociation zone in the annulus of transition from the density-bounded HII region on the near side to the ionization-bounded situation on the far side. The components of this model are illustrated in the cross-section shown in Fig. 12. Models of HI dissociation zones associated with O and early B stars, such as those of Roger & Dewdney (1992), apply to ionization-bounded systems and follow the advancement of the dissociation front into the surrounding molecular gas ahead of the ionization. For Sh170 this situation would initially prevail in directions from the star toward the dense molecular cloud. However, the models show that for an O9V star and densities near 1000 nucleons cm$^{-3}$ any dissociation zone in the dense gas would be short lived because of the intensity of the radiation, the ionization front merging with the dissociation front in a time $\leq 2 \times 10^5$ years. On the other hand, in the suggested annular transition zone on the periphery of the ionization cone, where densities and density gradients would be much less, one could expect a dissociation zone ahead of the ionization front to persist for as long as $10^6$ years. Much of the dissociated hydrogen may be caught up by a shock front preceding the expanding ionization front (cf. Franco et al. 1990; Rodríguez-Gasper et al. 1995). A similar phenomenon is apparent in the observations of the prominent HI dissociation region associated with IC 5146 (Roger & Irwin 1982), where the supposed champagne flow is confined to a

narrower cone than is the case for Sh170. For IC 5146 a clear ring of HI emission can be seen with an expansion velocity of $\sim$2.5 km s$^{-1}$ relative to the bulk of the emission. The HI dissociation zones of Sh187 (Joncas et al. 1992) and NGC 281 (Roger & Pedlar 1981) also show clear signatures of expansion. Similarly, van der Werf & Goss (1989) show that components of the HI emission associated with Orion A have expansionary velocities and discuss various mechanisms for neutral gas movement at the periphery of an ionized component.

If the geometry of the components of Sh170 is similar to that depicted in Fig. 12, our inability to detect any signature of outward expansion in the observations of HI would be explained by the motion being largely transverse to the line-of-sight. Nevertheless, noting the similarities to the expanding HI zones cited above, and the appearance of parts of the HI boundary which follows at a larger radius the circular boundary of the ionized gas, (cf. Figs. 3 and 5), we consider it likely that much of the HI is expanding outwards, possibly driven by the pressure of the HII region. However, it is possible that up to 30% of the HI within the ellipse in Fig. 5 is part of the pre-existing, underlying distribution connected via the bridges on the north and west sides of Sh170. If this is the case, the amount of associated HI listed in Table 2 should be reduced.

### 5.3. The molecular cloud

We see the molecular cloud as a dense concentration which has formed in the band of atomic hydrogen, parts of which extend as lanes of emission to the north and west of Sh170.

From our estimates, the molecular cloud as depicted by the CO emission, is approximately one-half the mass of the original cloud before photo-evaporation commenced. Since the probable time-scale of the present erosion represents less than one-tenth of the expected main-sequence lifetime for an O9V star, total disruption of the cloud by this star would seem inevitable. This conclusion is in accord with calculations of cloud disruption in models of blister regions and champagne flow (e.g. Rodríguez-Gasper et al. 1995).

Our view of the molecular cloud is derived from the maps of the emissions from CO and from dust, both minor components. Some studies of HI, CO and far-infrared emissions in interstellar cirrus clouds (e.g. Reach et al. 1994) suggest that a substantial component of $H_2$ may exist in diffuse regions where no CO can be detected. This could be due to differences in the formation and destruction rates for the CO and $H_2$ molecules, to differences in the shielding properties, or to insufficient excitation of CO in the lower density gas. Although we have found no direct evidence to support the existence of such a "concealed" component in the Sh170 complex, it is possible that clumps of $H_2$, intermixed on a large scale with the HI, could explain the lack of a detailed pixel-by-pixel correlation between the atomic component and the dust emission.

## 6. Summary

We have presented observations at arc-minute resolution of the ionized, atomic, molecular and dust components in the region of Sh170. The observations show the single exciting star to be centrally located on the near side of a small isolated molecular cloud, in projection just inside its southern boundary. The emission from the extended ionized gas shows it to be almost circular in outline, approximately centred on the star, with a mean velocity of approach with respect to that of the molecular cloud. The HI emission shows most of the atomic component to be within a radius about 40% greater than that of the HII but to have a mean radial velocity similar to that of the molecular gas. The range in radial velocity of the HI emission, however, is more than 2.5 times that of the CO emission. The far-infrared emission shows dust components coexistent with both the extended HI and the compact CO cloud.

We suggest that the HII region is an example of on-going ionized flow from the front surfaces of the molecular cloud. If the star is as close to the cloud as it appears in projection, it is likely that ablation of the cloud continues to add material to the outflowing ionized gas. About 40% of the total mass of the complex is in atomic (HI) gas and we propose that much of this dissociated component is in an annular zone, beyond the ionization front in directions from the star roughly transverse to the line-of-sight, between the conical ionized outflow region on the near side of the star and a presumed density-bounded region on the far side of the star toward the molecular cloud. This zone would subtend a substantial solid angle and may be an important factor in the dispersal of the molecular cloud. The Sh170 complex is one of several young HII-HI-$H_2$ regions with similar characteristics. A more quantitative understanding of these regions requires new models which can track the production and dynamics of both the ionized *and* dissociated components, particularly for stars and HII regions in the density gradients on the boundaries of molecular clouds. In addition, new higher-resolution observations, particularly of the molecular components of Sh170, might provide direct evidence of a dynamical link between the suggested ionization front and the dense cloud.

*Acknowledgements.* We thank the MWO for generously providing observing time. D. Giguere, D. Blouin and A. Krider assisted at various stages of the data reduction. We are also indebted to L. Higgs for reduction software, J. Galt for assistance with broad-structure HI observing, and to D. Turner for discussions on the distance to the nebula. We thank the referee for numerous suggestions which have improved the clarity of the paper. The Canadian Galactic Plane Survey is a Canadian project with international partners, and is supported by the Natural Sciences and Engineering Research Council of Canada.

## References

Andersson, B.-G., Roger, R. S., & Wannier, P. G. 1992, A&A, 260, 355
Bertoldi, F., & Draine, B. T. 1996, ApJ, 458, 222
Bodenheimer, P., Tenorio-Tagle, G., & Yorke, H. W. 1979, ApJ, 233, 85
Bohlin, R. C., Savage, B. D., & Drake, J. F. 1978, ApJ, 224, 132
Boulanger, F. 1999, Dust Emission and ISM Components in New Perspectives on the Interstellar Medium, ed. A. R. Taylor, T. L. Landecker, & G. Joncas, ASP Conf. Ser., 168, 173
Boulanger, F., Abergel, A., Bernard, J.-P., et al. 1996, A&A, 312, 256
Brunt, C., & Ontkean, X. 2003, in preparation

Casoli, F., Dupraz, C., Gerin, M., Combes, F., & Boulanger, F. 1986, A&A, 169, 281
Crampton, D., & Fisher, W. A. 1974, Pub. D.A.O., 14 (12)
Clark, B. G. 1980, A&A, 89, 377
Combes, F. 1991, ARA&A, 29, 195
Dewdney, P. E., Roger, R. S., Purton, C. R., & McCutcheon, W. H. 1991, ApJ, 370, 243
Diaz-Miller, R. I., Franco, J., & Shore, S. N. 1998, ApJ, 501, 192
Digel, S. W., Grenier, I. A., Heithausen, A., Hunter, S. D., & Thaddeus, P. 1996, ApJ, 463, 609
Draine, B. T., & Lee, H. M. 1984, ApJ, 285, 89
Felli, M., & Harten, R. H. 1981, A&A, 100, 42
Franco, J., Tenorio-Tagle, G., & Bodenheimer, P. 1990, ApJ, 349, 126
Franco, J., Shore, S. N., & Tenorio-Tagle, G. 1994, ApJ, 436, 795
Georgelin, Y. M., Georgelin, Y. P., & Roux, S. 1973, A&A, 25, 337
Hartmann, D., & Burton, W. B. 1997, Atlas of Galactic Neutral Hydrogen (Cambridge University Press)
Heyer, M. H., Brunt, C., Snell, R. L., et al. 1998, ApJS, 115, 241
Higgs, L. A., & Tapping, K. F. 2000, AJ, 120, 2471
Hollenbach, D. J., & Tielens, A. G. G. M. 1999, Rev. Mod. Phys., 71, 173
Hunter, D. A., & Massey, P. 1990, AJ, 99, 846
Israel, F. P. 1978, A&A, 70, 769
Joncas, G., Durand, D., & Roger, R. S. 1992, ApJ, 387, 591
Joncas, G., & Roy, J. R. 1986, ApJ, 307, 649
Kutner, M. L., & Leung, C. M. 1985, ApJ, 291, 188
Lahulla, J. F. 1985, A&AS, 61, 537
Landecker, T. L., Dewdney, P. E., Burgess, T. A., et al. 2000, A&AS, 145, 509
Mayer, P., & Macák, P. 1973, Bull. Astron. Inst. Czech., 24, 50
Miville-Duchênes, M.-A., Joncas, G., & Durand, D. 1995, ApJ, 454, 316
Panagia, N. 1973, AJ, 78, 929
Reach, W. T., Koo, B.-C., & Heiles, C. 1994, ApJ, 429, 672
Rodríguez-Gasper, J. A., Tenorio-Tagle, G., & Franco, J. 1995, ApJ, 451, 210
Roger, R. S. 2002, Seeing Through the Dust: The Detection of HI and the Exploration of the ISM in Galaxies, ed. A. R. Taylor, T. L. Landecker, & A. G. Willis, ASP Conf. Ser., 276, 260
Roger, R. S., Costain, C. H., Lacey, J. D., Landecker, T. L., & Bowers, F. K. 1973, Proc. IEEE, 61, 1270
Roger, R. S., & Dewdney, P. E. 1992, ApJ, 385, 536
Roger, R. S., & Irwin, J. A. 1982, ApJ, 256, 127
Roger, R. S., & Pedlar, A. 1981, A&A, 94, 238
Sanders, D. B., Solomon, P. M., & Scoville, N. Z. 1984, ApJ, 276, 182
Schraml, J., & Mezger, P. G. 1969, ApJ, 156, 269
Steer, D. G., Dewdney, P. E., & Ito, M. R. 1984, A&A, 137, 159
Taylor, A. R., Gibson, S. J., Peracaula, M., et al. 2003, AJ, 125, 3145
Tenorio-Tagle, G. 1979, A&A, 71, 59
Vacca, W. D., Garmany, C. D., & Shull, J. M. 1996, ApJ, 460, 914
van der Werf, P. P., & Goss, W. M. 1989, A&A, 224, 209
Warin, S., Benayoun, J. J., & Viala, Y. P. 1996, A&A, 308, 535
Yorke, H. W., Bodenheimer, P., & Tenorio-Tagle, G. 1982, A&A, 108, 25